International Journal of Swarm Intelligence and Evolutionary Computation

Sri Madhava Raja et al., Int J Swarm Intel Evol Comput 2014, 3:1
DOI: 10.4172/2090-4908.1000107

Research Open Access

# Analysis of Vasculature Detection in Human Retinal Images Using Bacterial Foraging Optimization Based Multi Thresholding

**N Sri Madhava Raja[1]*, G Kavitha[2] and S Ramakrishnan[3]**

[1]*Department of Electronics and Instrumentation Engg., St. Joseph's College of Engineering, OMR, Chennai, Tamil Nadu, India*
[2]*Department of Electronics Engineering, M.I.T. Campus, Anna University, Chennai, Tamil Nadu, India*
[3]*Biomedical Engineering Group, Department of Applied Mechanics, Indian Institute of Technology Madras, Chennai, Tamilnadu, India*

## Abstract

Analysis of blood vessels in digital retinal fundus images is an important problem attempted in contemporary biomedical engineering research. In this work, normal and abnormal retinal images are pre-processed with adaptive histogram equalization and fuzzy filtering. Pre-processed images are then subjected to Tsallis multi-level thresholding method. The threshold levels determined by the chosen method are further optimized using bacterial foraging optimization techniques in order to improve the vessel content. The obtained results are validated using similarity measures by comparing with the corresponding ground truth of each image. Statistical and Tamura features are derived from optimal multi-level thresholding output images to analyse the healthy and pathological images. Results demonstrate that attempted series of pre-processing techniques enhances the edge information considerably and improves the efficacy of segmentation. It is observed that bacterial foraging optimization for Tsallis multi-level thresholding is able to extract retinal vasculature. Similarity measures show that this method provides considerable improvement in the extraction of vessel edges. Further, the statistical and Tamura features derived from detected vessels provide better differentiation between healthy and pathological images. As presence and absence of vessels in retina are clinically significant, the findings seem to be useful.

**Keywords:** Retinal vasculature; Tsallis Multilevel thresholding; Bacterial foraging optimization (BFO); Similarity measures; Tamura features

## Introduction

The retina is the light sensitive, multi-layered sensory tissue of the eye. It is the inner and most important layer of the eye which receives images formed by the lens and transmits them through the optic nerve to the brain. Retina comprises various significant anatomical structures such as optic disc, blood vessels and macula. The retinal vasculature is an important part of the blood circulatory system that can be observed directly and a number of systemic conditions can be diagnosed by the detection of lesions in the retinal vasculature. Changes in these structures correlate with pathological changes and provide information on severity or state of various diseases such as diabetes, arteriosclerosis, hypertension and coronary heart disease [1].

Image processing, analysis and computer vision techniques are increasing in prominence in medical science, especially ophthalmology. Existing development in image processing relevant to ophthalmology iims (Ns), maxludes the progress made towards developing automated diagnostic systems for conditions such as diabetic retinopathy, age-related macular degeneration and retinopathy of prematurity [2]. These diagnostic systems offer the potential to be used in large-scale screening programs, with reduced human intervention [3]. Optic fundus photography technique is a widely used procedure to image retinal fundus which indicates the optic disc, vessel tree and macula.

Automated segmentation of the vessels is the first step in the analysis of retinal vascular system. Vessel segmentation can be used to study the correlation between the micro vascular system and health. Survey of the different techniques related to vessel detection has been proposed by Kirbas and Quek [4]. Chaudhuri et al. have proposed a two-dimensional linear kernel with a Gaussian profile for segmentation of the vasculature [5]. Existing methods for vessel segmentation in retinal images are based on intensity edges, matched filters, adaptive thresholding, modified active shape model and wavelets [6,7]. It has been found that the extraction of vessels is a strenuous task to perform [3]. In a retinal image, vessels are darker than their surroundings. Many structures in the retina show similar intensity values similar to that of vessels values in pathological conditions. Also, difficulties occur in identification of vessels due to bifurcations or branching due to calcification.

Recently, evolutionary algorithms such as genetic algorithm (GA), differential evolutions, tabu search, Particle Swarm Optimization (PSO) and Ant Colony Optimization (ACO) have found wide spread application. PSO is an evolutionary computation technique, based on bird flocking and fish schooling [8]. The Bacterial Foraging Optimization (BFO) algorithm is inspired from forage of food by Escherichia coli bacteria and is a robust algorithm for non – gradient optimization solution [9]. In this scheme, the foraging behaviour of Escherichia coli bacteria present in our intestines is mimicked [10]. It is used to solve various engineering problems such as harmonic estimation and transmission loss reduction [11,12]. A bacterial foraging optimization algorithm for multilevel thresholding has been applied to MR brain images [13].

The clinical usefulness and diagnostic accuracy of a retinal image is highly dependent on its performance to segment the object of interest accurately and thereby quantification is important. Several measures

***Corresponding author:** N Sri Madhava Raja, Department of Electronics and Instrumentation Engg., St. Joseph's College of Engineering, Chennai, Tamil Nadu, India, Tel: 044 2257 5052; E-mail: nsrimadhavaraja@stjosephs.ac.in

**Received** October 16, 2013; **Accepted** December 30, 2013; **Published** January 15, 2014

**Citation:** Sri Madhava Raja N, Kavitha G, Ramakrishnan S (2014) Analysis of Vasculature Detection in Human Retinal Images Using Bacterial Foraging Optimization Based Multi Thresholding. Int J Swarm Intel Evol Comput 4: 107. doi: 10.4172/2090-4908.1000107

are used to quantify the similarity between the segmentation results with respect to different criteria [14]. Recently, a framework for evaluation of image segmentation based on the similarities of image intensity and boundary shape for medical images has been proposed [15].

Methods used in extracting features for classification include run-length statistics, co-occurrence matrices and statistical moments. The first order statistical parameters consider the property of gray level and second order statistics deals with spatial distribution of gray levels. Typical statistical measures used in classification are mean, standard deviation, energy, entropy, skewness, kurtosis, contrast, homogeneity, dissimilarity, variance, correlation, maximum probability, cluster tendency and inverse difference moment [16,17]. The ratio of vessel to vessel free area for both normal and abnormal retinal images was identified as Vessel Density Index (VDI) [18]. The tamura texture features coarseness, contrast, directionality, line likeness, regularity, and roughness are used in image retrieval [19].

In this work, bacterial foraging optimization algorithm based multilevel threshold is adopted for detecting the vasculature structures in retinal fundus image. Initially, adaptive histogram equalization and clique function are used for pre-processing of original images [20]. The initial multilevel threshold levels are obtained using Tsallis technique [21]. The optimized threshold levels are obtained using bacterial foraging technique to improve the segmentation of vessels. Different features are extracted from the segmented results to differentiate healthy and pathological subjects. The features considered for analysis in this work include VDI, energy, entropy, contrast, line likeness and directionality which are used to differentiate normal and pathological subjects.

## Methodology

The DRIVE [22] database has been used in this work for segmentation of blood vessels in retinal images. In the proposed method, adaptive histogram equalisation technique has been considered for the enhancement of the image quality. Further, local statistics is determined at the pixel position (i,j) and is a function of a local group of pixels called the clique [23]. Its value depends on the variation of image's intensity values on the eight neighbourhoods. It highlights the edge information of the vessels. Further to detect the information present in the image, Tsallis based thresholding method is attempted. This method is similar to the maximum entropy sum method of Djerou et al. [24].

Tsallis entropy criterion method is extended to multi-level thresholding and is described as follows:

$$f(t) = argmax[s_q^A(t) + S_q^B(t) + (1-q)S_q^A(t).S_q^B(t)] \quad (1)$$

Where, q is an entropic index

$$S_q^A(t) = \frac{1 - \sum_{i=0}^{t-1}\left(\frac{P_i}{P^A}\right)^q}{q-1}, \quad P^A = \sum_{i=0}^{t-1} P^i \quad (2)$$

$$S_q^B(t) = \frac{1 - \sum_{i=0}^{t-1}\left(\frac{P_i}{P^B}\right)^q}{q-1}, \quad P^B = \sum_{i=0}^{t-1} P^i \quad (3)$$

This Tsallis entropy criterion method can also be extended to multilevel thresholding and is described as follows:

$$f(t) = [S_q^A(t) + S_q^B(t) + S_q^C(t) + \ldots + S_q^M(t) + (1-q)S_q^A(t)S_q^B(t)S_q^C(t)\ldots S_q^M(t)]$$

where, $S_q^A(t)\, S_q^B(t)\, S_q^C(t)\, S_q^M(t)$ is represented similar to Eq.2.

The aim of this proposed BFO algorithm is to maximize the Tsallis objective function using entropy equations. The information measures between the two classes (object and background) are maximized. When $S_q^A(t)$ is maximized, the luminance level t is considered to be the optimum threshold value. The performance of the algorithm is improved by selection of optimized multilevel thresholds by applying BFO algorithm.

## Implementation of BFO for multilevel thresholding problem

In bacterial foraging technique introduced by Passino [10], a set of bacteria tries to reach an optimum threshold value by following stages namely chemotaxis, swarming, reproduction, elimination and dispersal. Each bacterium produces a solution iteratively for a set of optimal values of parameters. Gradually, all the bacteria converge to the global optimum threshold value. In the chemotaxis stage, the bacteria have an option to tumble followed by a tumble or a tumble followed by a run or swim. The movement of bacteria is accomplished through swimming and tumbling. In swarming, each *E. coli* bacterium signals another bacterium via attractants to swarm together. In the reproduction stage, the least healthy bacteria die. The healthiest, bacterium splits into two bacteria and are placed at the same location. While in the elimination and dispersal stage, any bacterium is either eliminated or dispersed from the set to a random location during the optimization. This

| SUT (Y) | Ground truth (X) | | |
|---|---|---|---|
| | 1 | 0 | sum |
| **1** | a | b | a+b |
| **0** | c | d | c+d |
| **Sum** | a+c | b+d | a+b+c+d |

**Table 1:** Contingency table values.

| Sl.No | Similarity measure | Formula |
|---|---|---|
| 1 | Simple matching | $\frac{a+d}{a+b+c+d}$ |
| 2 | Rogers and Tanimoto | $\frac{a+d}{a+d+2(b+c)}$ |
| 3 | Hamann measure | $\frac{(a+d)-(b+c)}{a+b+c+d}$ |
| 4 | Sokal and Sneath-II | $\frac{2(a+d)}{2(a+d)+b+c}$ |
| 5 | Jaccard measure | $\frac{a}{a+b+c}$ |
| 6 | Anderberg measure | $\frac{t_1-t_2}{2(a+b+c+d)}$ |
| 7 | Czekanowsky | $t_1$=max(*a*,*b*) + max(*c*,*d*) + max(*a*,*c*) + max(*b*,*d*)<br>$t_2$=max(*a*+*c*, *b*+*d*) + max(a+b, *c*+*d*)<br>$\frac{2a}{2a+b+c}$ |
| 8 | Braun and Banquet | $\frac{a}{\max(a+b,a+c)}$ |
| 9 | Pearson and Heron-II | $\frac{ad-bc}{\sqrt{(a+b)(a+c)(b+d)(c+d)}}$ |
| 10 | Baroni-Urbani and Buser-I | $\frac{\sqrt{ad}+a}{\sqrt{ad}+a+b+c}$ |
| 11 | Baroni-Urbani and Buser-II | $\frac{\sqrt{ad}+a-(b+c)}{\sqrt{ad}+a+b+c}$ |

**Table 2:** Binary similarity measure.

stage mainly prevents the bacteria from attaining the local optimum. If h represents the position of a bacterium and J(h) the value of the objective function, then the conditions J(h) < 0, J(h) = 0, and J(h) > 0 indicates if the bacterium at location h is in nutrient-rich, neutral and toxic environments, respectively. Basically, chemotaxis is a foraging behaviour where bacteria tries to climb up the nutrient concentration to find the lower values of J(h) and avoid toxic substances. They search for ways out of neutral media. The BFO algorithm is modified to find the optimum thresholds suitable for detection of anatomical structures in the retina. The search space for bacteria consists of searching for four optimal thresholds for segmentation of blood vessels in the image.

The algorithm starts with the calculation of objective value using equation (2) for the initial bacterial population inside the innermost chemotaxis loop. Any $i^{th}$ bacteria at the $j^{th}$ chemotactic, $k^{th}$ reproduction and $l^{th}$ elimination stage is θi (j,k,l) and its corresponding objective value is given by $J_1$(i,j,k,l).

$$\theta^i(j+1,k,l)=\theta^i(j,k,l)+C(i)\frac{\Delta(i)}{\sqrt{\Delta^T(i)\Delta(i)}} \quad (4)$$

The BFO algorithm is used to find the optimal retinal vessels in the fundus image. The search space for bacteria consists of searching four optimal thresholds for segmentation of blood vessels in the image.

## Similarity measures

In this work, eleven similarity measures are used to quantify the similarity between segmentation and ground truth. It creates a hierarchical cluster tree using ward inner squared distance or min variance algorithm. Segmentation under test is the segmentation that has an unknown evaluation and reference segmentation is the segmentation with a known evaluation [25].

Let $X_{i,j}$ be the pixel corresponding to ground truth and $Y_{i,j}$ be the pixel corresponding to the Segmented image Under Test (SUT) then

a = number of times $X_{i,j}$=1 and $Y_{i,j}$=1

b = number of times $X_{i,j}$=0 and $Y_{i,j}$=1

c = number of times $X_{i,j}$=1 and $Y_{i,j}$=0

d = number of times $X_{i,j}$=0 and $Y_{i,j}$=0

Table 1 show the contingency values used in similarity measure calculation. Simple matching similarity measure is the ratio of the number of matches to the total number of characteristics. Jaccard similarity measure is also known as the similarity ratio. Kulczynski-II similarity measure gives the average conditional probability that a characteristic is present in one item given that the characteristic is present in the other item. Sokal and Sneath similarity measure-IV is the conditional probability that a characteristic of one item is in the same state (present or absent) as the characteristic of the other item. This measure is an average over both items acting as predictors. Hamann similarity measure gives the probability that a characteristic has the same state in both items (present in both or absent from both) minus the probability that a characteristic has different states in the two items

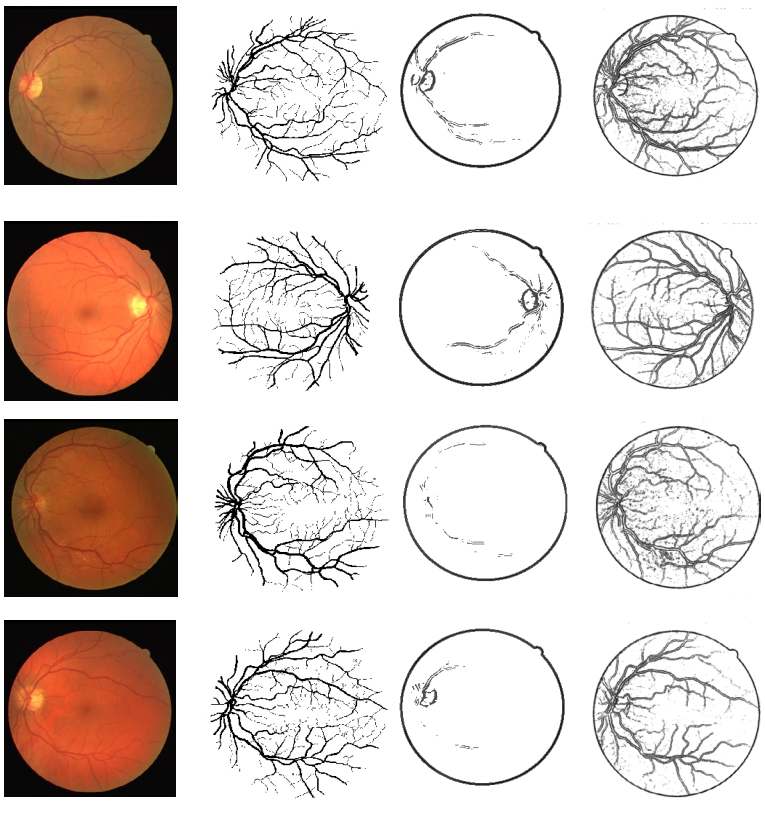


**Figure 1:** a) Representative normal retinal (b) corresponding ground truth (c) Segmentation result of Tsallis based multithreshold method and (d) Segmentation result of Bacterial foraging optimisation based multi-threshold method.

(present in one and absent from the other). It is monotonically related to simple matching, Rogers and Tanimoto. Ochiai-I similarity measure is the binary form of the cosine. Pearson and Heron-I is the binary form of the Pearson product-moment correlation coefficient. All the similarity measures have the range of 0 to 1 except Hamann, which has the range of -1 to +1.

Table 2 shows the various similarity measures and their formulae. Analysis of these similarity measures is performed with dendrogram plot. The plot shows dependence of various similarity measures with cluster formations between the interdependent data. Further, analysis of the retinal image is performed with several features. Vessel density index is derived based on the presence and absence of vessel detected.

In addition, features such as energy, contrast, entropy, line likeness and directionality are also used for differentiating healthy and pathological subjects. Contrast is a measure of relative intensity between a pixel and its neighbour in relative location. Entropy is a measure of randomness of intensity image and characterizes the texture non-uniformity. Energy is a measure of intensity variation in the segmented region, which also represents the non-uniformity in the histogram. Directionality defines whether texture pallets are oriented in single direction or not representing directional or non-directional. The degree of directionality is measured using the frequency distribution of oriented local edges against their directional angles. Line-likeness corresponds to pattern elements, whether texture formed by lines are line-like or blob-like. It is the average coincidence of the edge directions that co-occurred in the pairs of pixels separated by a distance along the edge direction in every pixel. This edge strength is expected to be greater than a given threshold eliminating trivial weak edges. The coincidence measure is calculated by the cosine of difference between the angles, so that the co-occurrences in the same direction are measured by +1 and those in the perpendicular directions by -1 [26].

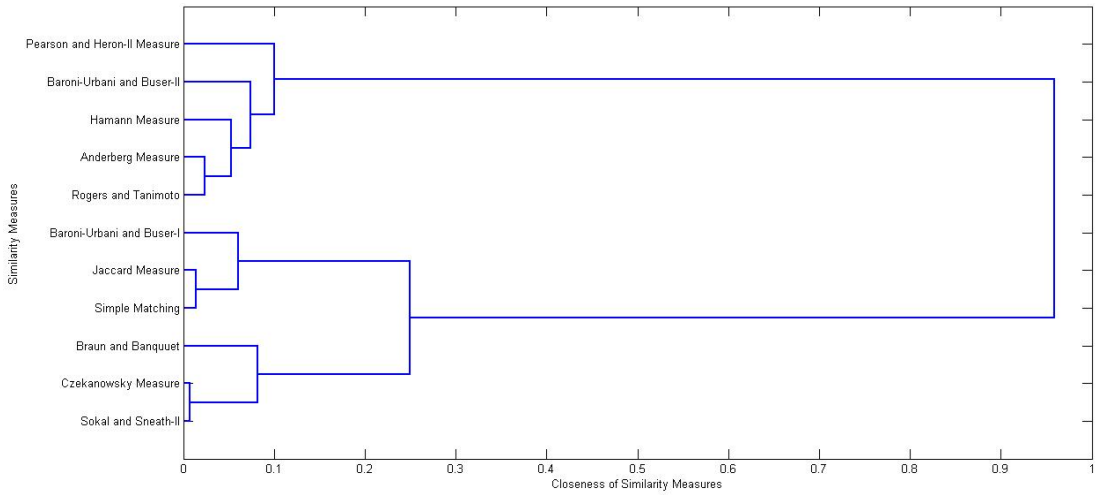


**Figure 2:** Dendrogram of similarity measures obtained from BFO based Tsallis multilevel threshold for normal images.

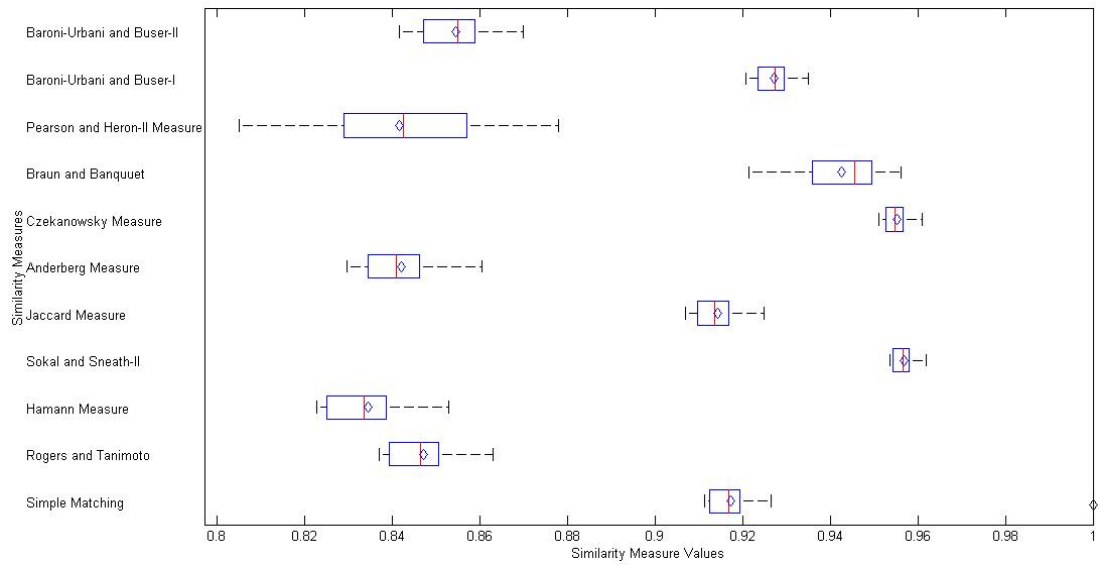


**Figure 3:** Box plot representation of the different similarity measures.

## Results and Discussion

In this work, normal and abnormal retinal samples from age matched, healthy and adult volunteers are obtained from DRIVE database and nearby hospitals for study. These retinal images are acquired through a high sensitive colour fundus camera with constant illumination, resolution, field of view, magnification and dilation procedures. Input images of same size (256 x 256) are considered for analysis.

The results obtained using multilevel thresholding with and without optimization procedure are shown in Figure 1 along with their corresponding ground truth images.

In this multi thresholding algorithm, the number of thresholds is selected properly such that it detects the high intensity large vessels, low intensity thinner vessels and still lower small vessels. In the proposed algorithm four threshold levels are selected to detect maximum vessel information.

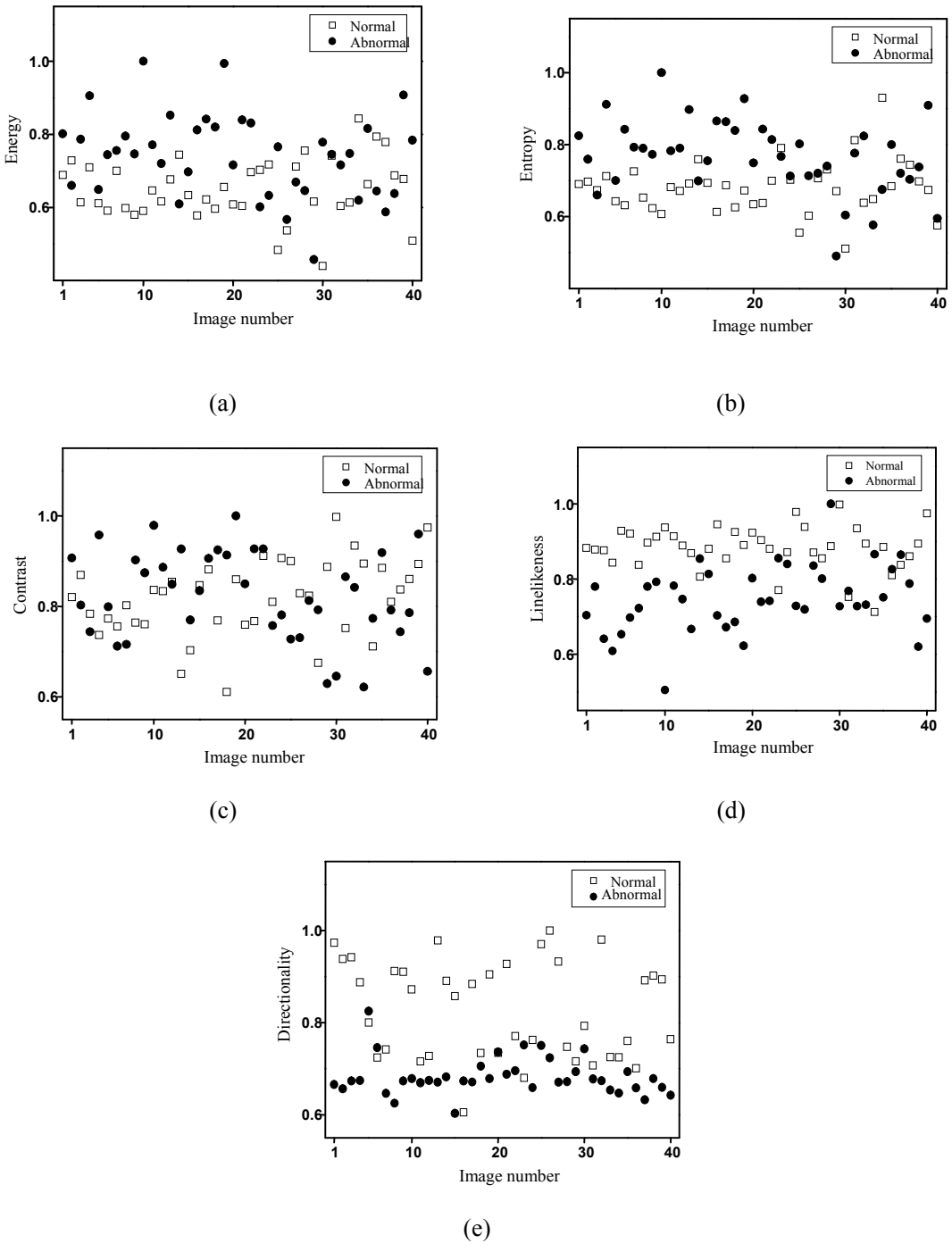


**Figure 4:** Variations of features for different normal and abnormal images (a) energy, (b) entropy, (c) contrast, (d) line-likeness and (e) directionality.

Figure 1a shows representative normal retinal images and its corresponding extracted ground truth is shown in Figure 1b. Figure 1c is segmented image using multilevel thresholding and Figure 1d shows image obtained using BFO based multithresholding. For the implementation of BFO algorithm, several parameters such as population size (S), maximum number of chemotactic steps ($N_c$), maximum number of swims ($N_s$), maximum number of reproduction steps ($N_{re}$) and maximum number of elimination-dispersal events ($N_{ed}$) are initialized. If the parameters S, $N_c$, $N_s$, $N_{re}$ and $N_{ed}$ are too small, the algorithm may converge prematurely; however, larger values of the parameters increase the computational complexity and also affect the solution quality. A general biologically inspired thumb-of-rule for choosing the parameters of BFO is: $N_c > N_{re} > N_{ed}$ [13]. The BFO algorithm is applied repetitively by considering different values of BFO key parameters such as $N_c$, $N_s$, $N_{re}$ and $N_{ed}$. In this work $N_c$, $N_s$, $N_{re}$ and $N_{ed}$ are selected as 10, 5, 4 and 2 respectively.

The dendrogram shown in Figure 2 gives three distinct clusters of similarity measures for detection of retinal blood vessels using optimal thresholds. The cluster 1 includes the Rogers and Tanimoto, Anderberg, Hamann, Baroni-Urbani & Buser-II, Pearson & Heron. These similarity measures range from 0.80 to 0.87. The similarity measures bundled in cluster 2 has the range of 0.90 to 0.93 and the measures are simple matching, Jaccard measure, Baroni-Urbani and Buser-I. The similarity measures corresponding to cluster 3 are Sokal and Sneath-II, Czekanowsky measure, Braun and Banquet measure. These clustered similarity measures have similar range (0.92 to 0.96) of similarity values.

Figure 3 represents the box plot obtained from various similarity measures obtained from comparing segmented vessels with their corresponding ground truths. Similarity measures belonging to first cluster namely Rogers and Tanimoto, Anderberg measure, Hamann measure, Baroni-Urbani & Buser-II and Pearson & Heron have mean values as 0.84, 0.84, 0.83, 0.85 and 0.84. In addition, similarity values of simple matching, Jaccard measure and Baroni-Urbani & Buser-I in second cluster have a mean value of 0.91, 0.92 and 0.92 respectively. Measures of third cluster include Sokal & Sneath-II, Czekanowsky measure and Braun & Banquet measures shows the mean values as 0.95, 0.95 and 0.94 respectively.

The features considered for analysis are energy, entropy, contrast, directionality and line-likeness. Further the variation of these features is represented by scattergram as shown in Figure 4. The energy value observed in Figure 4(a) is less in normal images compared to the pathological condition. This increase in contrast, representing the difference between the highest and the lowest values of contiguous set of values is due to the leaky blood vessels in the abnormal images. Because of lower bifurcations of retinal vessels in the normal images, entropy is observed to be more as shown in Figure 4b which indicates the non-uniformity in presence of vasculature. The higher the retinal vessel bifurcation in abnormal images, the higher is the contrast as shown in Figure 4c. This also represents the disorderliness or complexity of the retinal vessels in the abnormal images because of neo vasculature, leaky blood vessels and other symptoms.

Also, the line-likeness measure is observed to be high in abnormal images as shown in Figure 4d which represents the average coincidence of the pair of edge pixels in these images. This shows the uniform direction of the retinal vessels in the normal images. Since the frequency distribution of the oriented local edges in abnormal images is more, the degree of directionality is higher as shown in Figure 4e than normal images. Line-likeness and directionality features provides better differentiation between healthy and pathological subjects since more vessel information with piecewise linear segmented information are present in normal images.

## Conclusion

In this work, an attempt has been to detect and analyse retinal vasculature using BFO based multi-level thresholding method. The pre-processed BFO based Tsallis multi thresholding results in better detection of vasculature. The optimal multi threshold selection using BFO seems to provide more vessel information than without optimization procedure. Dendrogram analysis of the similarity measures show relevant information form clusters which is further used for validation of the algorithms. Features extracted from the optimally tuned output shows better differentiation of healthy and pathological subjects. Further, the results obtained could be used to address disorders such as diabetic retinopathy.

### References

1. Niall P, Tariq MA, Thomas MG,Ian JD, Baljean D, et al. (2006) Retinal Image analysis: Concepts applications and potential. Progress in Retinal and Eye Research 25: 99-127.
2. Carmen AL, Domenico T, Emanuele T (2010) FABC: Retinal Vessel Segmentation Using AdaBoost. IEEE Trans. On Info. Tech. in Biomedicine 14: 1267-1274.
3. Abràmoff MD (2010) Retinal Imaging and Image Analysis. IEEE Reviews in Biomed Engg 3: 169-208.
4. Kirbas C, Quek FKH (2003) Vessel Extraction Techniques and Algorithms: A Survey, Third IEEE Symposium on Bioinformatics and Bio Engineering.
5. Chaudhuri S, Chatterjee S, Katz N, Nelson M, Goldbaum M (1989) Detection of blood vessels in retinal images using two – dimensional matched filters. IEEE trans. on Med. Imag 8: 263-269.
6. Hoover A, Kouznetsova V, Goldbaum M (2000) Locating blood vessels in retinal images by piecewise threshold probing of a matched filter response. IEEE Trans. Med. Imaging 19: 203-210.
7. Opas C (2006) Fundus Foveal Localization Based on Vessel Model, Proceedings of the 28th IEEE EMBS Annual International Conference New York City, USA: 4440-4444.
8. Kennedy J, Eberhart R (1995) Particle Swarm Optimization, Proc. of IEEE Int. Conf. on Neural Networks. IV. 1942-1948.
9. Passino KM (2002) Biomimicry of bacterial foraging for distributed optimization and control. Control Systems Magazine, IEEE 22: 52-67.
10. Passino KM (2010) Bacterial Foraging Optimization, Int. J. Swarm Intelligence Research 1: 1-16.
11. Mishra S, Bhende CN (2007) Bacterial Foraging Technique-Based Optimized Active Power Filter for Load Compensation. IEEE Transactions on Power Delivery 22: 457-465.
12. Tang WJ, Li MS, Wu QH, Saunders JR (2008) Bacterial Foraging Algorithm for Optimal Power Flow in Dynamic Environments. IEEE Transactions on circuits and systems 55: 2433-2442.
13. Sathya PD, Kayalvizhi R (2011) Amended bacterial foraging algorithm for multilevel thresholding of magnetic resonance brain images. Measurement 44: 1828-1848.
14. Frounchi K, Lionel CB, Leo G, Yvan L, Rajesh S (2011) Automating image segmentation verification and validation by learning test oracles. Information and Software Technology 53: 1337-1348.
15. Satoko T, Hideo Y (2011) Algorithm Selection Based on a Region Similarity Metric for Intracellular Image Segmentation. Image Segmentation 419-434.
16. Ion AL (2009) Methods for knowledge discovery in images. Int. Conf on Inf. Technol 38: 1.
17. Ozdemir I, Norton DA,Ozkan UY, Mert A, Senturk O (2008) Estimation of Tree

Size Diversity Using Object Oriented Texture Analysis and Aster Imagery. Sensors 8: 4709-4724.

18. Sri Madhava Raja N, Kavitha G Ramakrishnan S (2011) Assessment of Retinal Vasculature Abnormalities using Slantlet Transform based Digital Image Processing. Biomedical Sciences Instrumentation 47: 88-93.
19. Deselaers T, Keysers D, Ney H (2008) Features for Image Retrieval: An Experimental Comparison. Information Retrieval 11: 77-107.
20. Mohanalin J, Kalra PK, Kumar N (2009) Tsallis Entropy Based Contrast Enhancement of Microcalcifications. Int. Conf. on Signal Acquisition and Processing 3-7.
21. Pizer SM, Amburn EP, Austin JD, Cromartie R, Geselowitz A (1987) Adaptive Histogram Equalization and Its Variations. Computer Vision, Graphics, and Image Processing 39: 355-368.
22. Staal JJ, MD Abramoff, Niemeijer M, Viergever MA, Van Ginneken B (2004) Ridge based vessel segmentation in color images of the retina. IEEE Trans. on Med. Imag. 23: 501-509.
23. Guowei W, Aiping W, Sikun L, Liang Z (2008) Solving stereo correspondence through minimizing energy function with higher-order cliques. International conference on Information and Automation 407-412.
24. Djerou L, Khelil N, Dehimi HE, Batouche M (2009) Automatic Multilevel Thresholding Using Binary Particle Swarm Optimization for Image Segmentation. International Conference of Soft Computing and Pattern Recognition 66-71.
25. Choi SS, Cha SH, Tappert C (2010) A Survey of Binary Similarity and Distance Measures. J. on Systemics, Cybernetics and Informatics 8: 43-48.
26. Guruprasad B, Biradar VG, Sarojadevi H, Nalini N (2012) Artificial Neural Network based Cancer Cell Classification. Comp. Engg. and Intelligent Systems 3: 2.

**Citation:** Sri Madhava Raja N, Kavitha G, Ramakrishnan S (2014) Analysis of Vasculature Detection in Human Retinal Images Using Bacterial Foraging Optimization Based Multi Thresholding. Int J Swarm Intel Evol Comput 4: 107. doi: 10.4172/2090-4908.1000107